SCIENTIFIC REPORTS

OPEN

SUBJECT AREAS:
MECHANICAL AND STRUCTURAL PROPERTIES AND DEVICES
CHEMICAL PHYSICS
MOLECULAR MACHINES AND MOTORS

Received
30 April 2014

Accepted
4 July 2014

Published
28 July 2014

Correspondence and requests for materials should be addressed to J.L. (lijingyuan@ihep.ac.cn); Y.Z. (zhaoyuliang@ihep.ac.cn) or R.Z. (ruhongz@us.ibm.com)

Rotation Motion of Designed Nano-Turbine

Jingyuan Li[1], Xiaofeng Wang[1], Lina Zhao[1], Xingfa Gao[1], Yuliang Zhao[1,4] & Ruhong Zhou[2,3,5]

[1]CAS Key Laboratory for Biomedical Effects of Nanomaterials and Nanosafety, Institute of High Energy Physics, Chinese Academy of Sciences, Beijing, 100049, China, [2]IBM Thomas J. Watson Research Center, Yorktown Heights, New York 10598, [3]Department of Chemistry, Columbia University, New York, New York 10027, [4]CAS Key Laboratory for Biomedical Effects of Nanomaterials and Nanosafety, National Center for Nanoscience and Technology of China, Beijing, 100190, China, [5]Institute of Quantitative Biology and Medicine, SRMP and RAD-X, Soochow University Medical College; Jiangsu Provincial Key Laboratory of Radiation Medicine and Protection, Suzhou 215123, China.

Construction of nano-devices that can generate controllable unidirectional rotation is an important part of nanotechnology. Here, we design a nano-turbine composed of carbon nanotube and graphene nanoblades, which can be driven by fluid flow. Rotation motion of nano-turbine is quantitatively studied by molecular dynamics simulations on this model system. A robust linear relationship is achieved with this nano-turbine between its rotation rate and the fluid flow velocity spanning two orders of magnitude, and this linear relationship remains intact at various temperatures. More interestingly, a striking difference from its macroscopic counterpart is identified: the rotation rate is much smaller (by a factor of ~15) than that of the macroscopic turbine with the same driving flow. This discrepancy is shown to be related to the disruption of water flow at nanoscale, together with the water slippage at graphene surface and the so-called "dragging effect". Moreover, counterintuitively, the ratio of "effective" driving flow velocity increases as the flow velocity increases, suggesting that the linear dependence on the flow velocity can be more complicated in nature. These findings may serve as a foundation for the further development of rotary nano-devices and should also be helpful for a better understanding of the biological molecular motors.

There are many nanoscopic machines in biological systems[1–7]. Among the most important functions of these motor proteins is to generate the rotational motion, e.g. F_0F_1-ATPase, flagella motor. With the development of modern nanotechnology, it becomes possible to design and construct functional artificial nanoscopic devices, resembling shuttles[8,9], turnstiles[10], cars[11,12], scissors[13], ratchets[14], and muscles[15]. There are many theoretical and experimental attempts to develop the nanomachine that can induce directional rotation as driven by electric or optical field[16–20]. Even though the fluid flow is very relevant and available, the design of nano-turbine that can be driven by fluid flow is still a challenge[21] and there are limited theoretical studies about the rotational behavior of flow-driven nano-turbine.

Here we present a designed nano-turbine constructed by a single-wall carbon nanotube (CNT) and graphene sheets. This nano-turbine can largely unidirectionally rotate as driven by a steady water flow. Despite many great progresses achieved in the development of nano-devices, the mechanism by which the nano-device works at nanoscale and the difference between the behavior of mechanical motion of a nano-device and its macroscopic analogue still largely remain elusive[22]. On the basis of the simulation of this designed model system, the rotation behavior of nano-turbine and the corresponding mechanism is studied in this work. We found the averaged rotation rate of the nano-turbine shows linear relationship with the flow velocity through two orders of magnitude. Compared to the macroscopic counterpart, the rotation rate of nano-turbine is much slower. Its efficiency of converting energy from fluid flow to the mechanical motion is only 6.4% of that of an ideal macroscopic counterpart. As indicated by the distribution of flow velocity, the "effective" driving flow velocity is remarkably smaller than the bulk flow velocity and the ratio can be as low as 0.15. The disruption of water flow, together with the water slippage at graphene surface and the dragging effect, should be related to the much slower rotation rate. It is interesting to note that the ratio of effective driving flow velocity decreases as the flow velocity increase, suggesting that the linear relationship between rotation rate and flow velocity may be more complicated. One possible explanation of the robust linear relationship between the rotation rate and flow velocity is that the other impacts, e.g. the water slippage and dragging, may get enhanced at the same time. Meanwhile, such linear relationship remains intact at different temperatures. On the other hands, the nano-turbine is found to rotate back-and-forth in small time period (less than 1 ns), but moves forward in the long run. The ratio of the standard

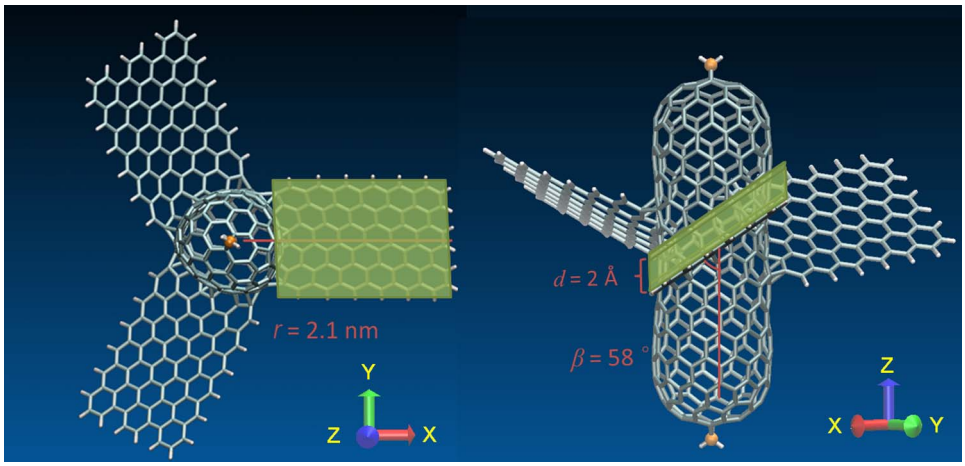

Figure 1 | The top view (left) and side view (right) of the designed nano-turbine placed along the z-axis, visualized with VMD[40]. The two fixed pole carbon atoms are shown as the golden balls. The rotation of nano-turbine is driven by the water flow along the – z-direction. The 2-Å slab above the turbine blade is shown as the green region.

deviation to the mean value of rotation period decreases as the flow velocity increases, and the relationship between them can be fit to the reciprocal of square root function very well.

Our results exhibit the stable linear dependence of rotation rate on the flow velocity, suggesting the nano-turbine can reliably reflect the flow velocity in various environments. Such nano-turbine should also have the application in rheology measurement. As indicated by our work, the significant thermal fluctuation at the nanoscopic length scale is important to the rotation behaviors of the nano-turbine. A sufficiently large blade is necessary for the nano-turbine to be effectively driven by the fluid flow, which should be considered in the future development of fluid flow driven nano-rotors. These findings might provide some insight for the further development of rotary nano-devices and should be helpful to a better understanding of the function of biological molecular motors, e.g. F_0F_1-ATPase, flagella motor[1–3,6], where the impact of thermal fluctuation is important to their function.

System and method

The designed nano-turbine is composed of the capped CNT and three graphene plates (Fig. 1). The (12,0) capped CNT with the length of 3.04 nm acts as the turbine axle. Three blades are made by the graphene plates covalently bonded to the CNT. The blades are parallel to the armchair direction of CNT, and the tilt angle, the angle between graphene plate and CNT axis β, is set to 58°. The dimension of graphene plate is 1.65×1.33 nm^2, and the radius of turbine $r = 2.1$ nm. The axle of turbine is placed along z-axis. The two carbon atoms at the poles of both ends of capped CNT are restrained to their initial positions respectively, so that the nano-turbine cannot be swept away by the water flow but is free to rotate across the axle. Experimentally, aromatic rings can be readily immobilized onto conjugated carbon surfaces using chemical reactions. For example, nitrobenzene can be mounted onto CNT side walls and graphene basal planes utilizing diazonium chemistry[23,24]. These chemical approaches may provide mechanics to realize the designed turbine experimentally, while the fabrication of well-structured nano-device might still be a challenge. Following our previous similar simulations on CNT-based system[25–27], the carbon atoms were modeled as uncharged Lennard–Jones particles with the $\sigma_{CC} = 0.34$ nm and $\varepsilon_{CC} = 0.3612$ kJ/mol. The designed nano-turbine was then solvated by the SPC/E water model. The dimension of the simulation system is $6.0 \times 6.0 \times 10.0$ nm^3. The rotation motion of nano-turbine in larger water box with the dimension of $9.0 \times 9.0 \times 15.0$ nm^3 is also studied. The directional water flow was achieved by applying an external force along -z direction to the water molecules. Six different flow velocities were tried to study the relationship between the rotation rate and the flow velocity. For each flow velocity, there are at least 50 rotation periods in the simulation to achieve the reliable average value of rotation rate. The corresponding simulation time ranges from 15 to 800 ns.

The molecular dynamics simulations were carried out at the constant pressure and constant temperature ensemble (NPT, 1 bar and 300 K) with gromacs 4.5 software package[28]. Velocity rescaling and Berendsen methods are used to control the temperature and pressure of system. Nose-Hoover thermostat method is also used for comparison. The rotational motion of the nano-turbine at both 300 K and 360 K was studied in this work. Periodic boundary conditions were applied in all three dimensions. The particle-mesh Ewald method was used to treat the long-range electrostatic interactions. A time step of 2 fs was used.

Results and discussion

Rotational motion of Nano-turbine. To achieve the directional water flow, an external force along -z direction is applied to the

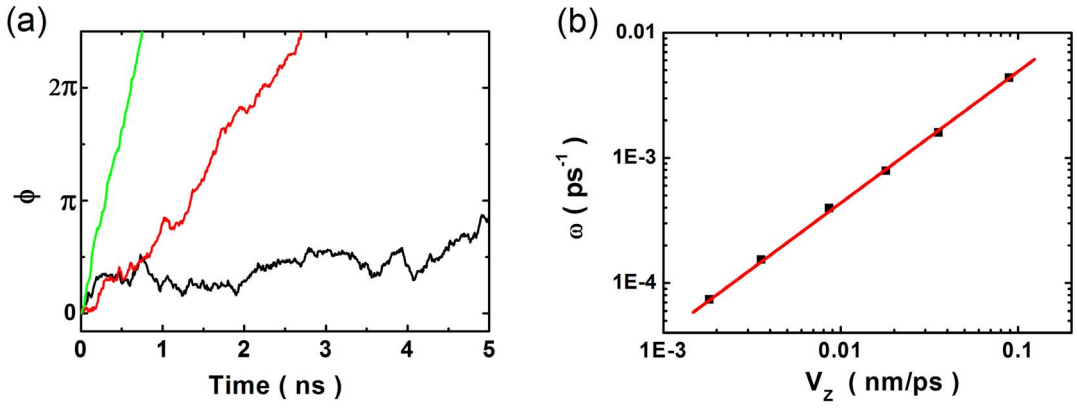

Figure 2 | Rotation motion of nano-turbine. (a) Examples of rotation motion of nano-turbine as characterized by φ, the angle between the rotor radius vector at time t with the vector at time 0. The rotation of nano-turbine is driven by the water flow of 1.82×10^{-3} (black), 8.63×10^{-3} (red) and 3.56×10^{-2} nm/ps (green). (b) The rotation rate of nano-turbine, ω, with respect to the average water velocity (denoted by flow velocity, V_Z) in 300 K. The relationship between them can be fit into a linear function very well: $\omega = -5.41 \times 10^{-5} + 0.0489 \times V_Z$ (red line).

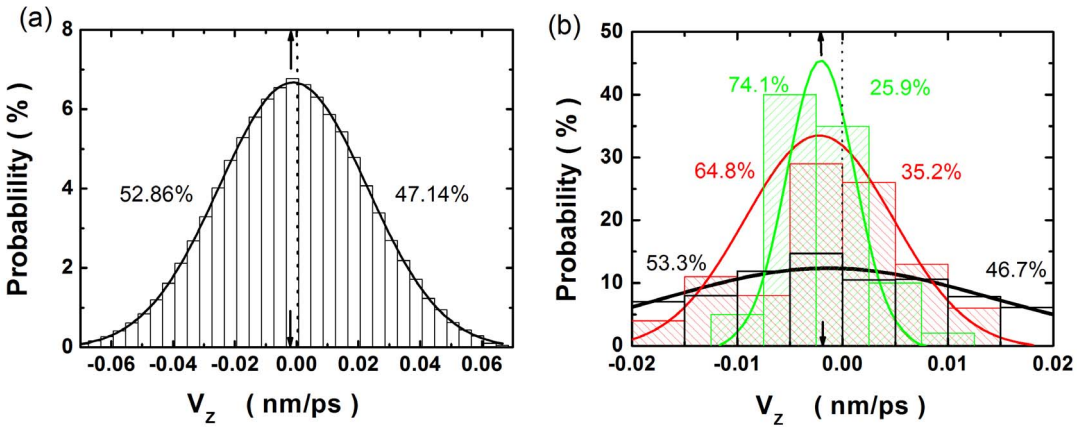

Figure 3 | The distribution of average velocity of water within 2-Å water slab in the system with the flow velocity of 1.82 × 10^{-3} nm/ps. (a) The fitting and the distribution of instant-average velocity of water (b) The fitting and the distribution of time-average velocity of water with the window size of 1 (black), 10 (red) and 50 ps (green).

water molecules. In this study, there are six acceleration rates have been used: 1 × 10^{-4}; 2 × 10^{-4}; 5 × 10^{-4}; 1 × 10^{-3}; 2 × 10^{-3}; 5 × 10^{-3} nm·ps^{-2}, corresponding to the osmotic pressure differences of 0.96, 1.92, 4.8, 9.6, 19.2, 48 Mpa (see more discussion in supplemental material)[25]. With the help of the external acceleration, the water flow along the -z direction is then generated. The averaged velocities in z-direction of bulk water are −1.82 × 10^{-3}, −3.63 × 10^{-3}, −8.63 × 10^{-3}, −1.8 × 10^{-2}, −3.56 × 10^{-2}, −8.9 × 10^{-2} nm/ps, respectively. The averaged water velocity is proportional to the acceleration rate, in agreement with the Navier-Stokes equation (see also Fig. S2). For convenience, we use the absolute value of the average water velocity in z-direction, V_Z, to represent the flow velocity in the following discussion. As driven by the water flow along the -z direction the designed nano-turbine rotates largely unidirectionally in counterclockwise (CCW) direction, i.e. the nano-turbine rotates in back-and-forth in an infinitesimal time period, but moves forward in the long run. We calculated the angle between the rotor radius vector at time t with the vector at time 0, $\phi(t)$, to characterize the rotational motion of turbine (Fig. 2(a)). For each flow velocity, there are at least 50 rotation periods in the simulation to achieve the reliable average value of rotation rate.

The nano-turbine rotates faster as the flow velocity increases. The rotation rate of nano-turbine, ω, has an almost perfect linear relationship with the flow velocity V_Z through two orders of magnitude (Fig. 2b). The fitted linear function is $\omega = -5.41 \times 10^{-5} + 0.0489 \times V_Z$, with a slope of 0.0489 nm^{-1}. Such linear relationship remains intact in the larger system with the size of 9 × 9 × 15 nm^3. Moreover, the dependence of rotation rate on the flow velocity appears insensitive to the choice of thermostat method. The result obtained from the simulations using Nose-Hoover thermostat also follows the linear relationship as in the systems using the Velocity-Rescaling thermostat (Fig. S3). This linear relationship resembles the linear dependence of the rotational rate of macro-scale water turbine on the driving flow velocity. For macro-scale water turbine this linear dependence can be described in terms of the momentum exchange with water flow. In the ideal situation, the turbine rotates at such a speed that the motion of the blade is on the same pace as the water flow. Thus, the ideal rotation rate of the macro-scale turbine can be derived from the geometric transformation of the water velocity, $\omega_i = (\tan \beta/r)\, V$, in which β is the tilt angle of blade, and r is the radius of turbine. In our system the value of $\tan \beta/r = 0.762$ nm^{-1}, which is

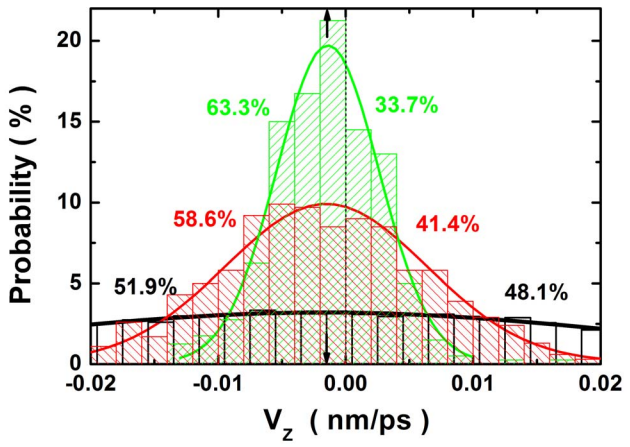

Figure 4 | The fitting and the distribution of time-average velocity of water within a smaller 2Å-slab with the window size of 1 (black) 10 (red) and 50 ps (green). The size of this water slab is 0.8 × 0.66 nm^2, one fourth of the blade size of the nano-turbine in this work.

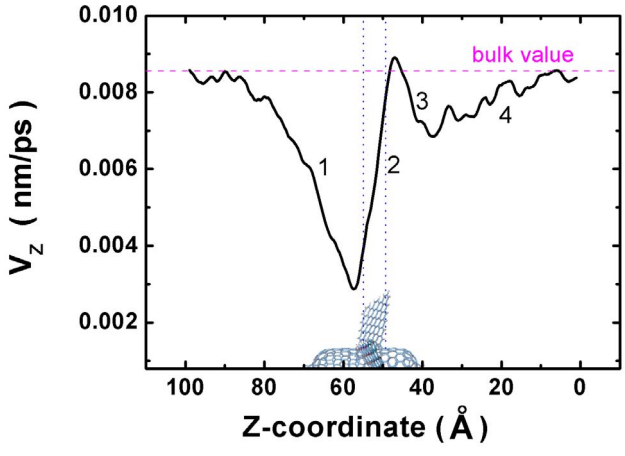

Figure 5 | The distribution of $V_{Z,locab}$ along the z-axis in the system with the flow velocity of −8.63 × 10^{-3} nm/ps. In the region above the turbine blade, the $V_{Z,local}$ decrease as the water get close to the blade (region 1); in the corresponding region of the blade (region 2) it increases sharply; then the $V_{Z,local}$ relaxes to 0.0069 nm/ps in region3 before it finally converges to the bulk value (region 4).

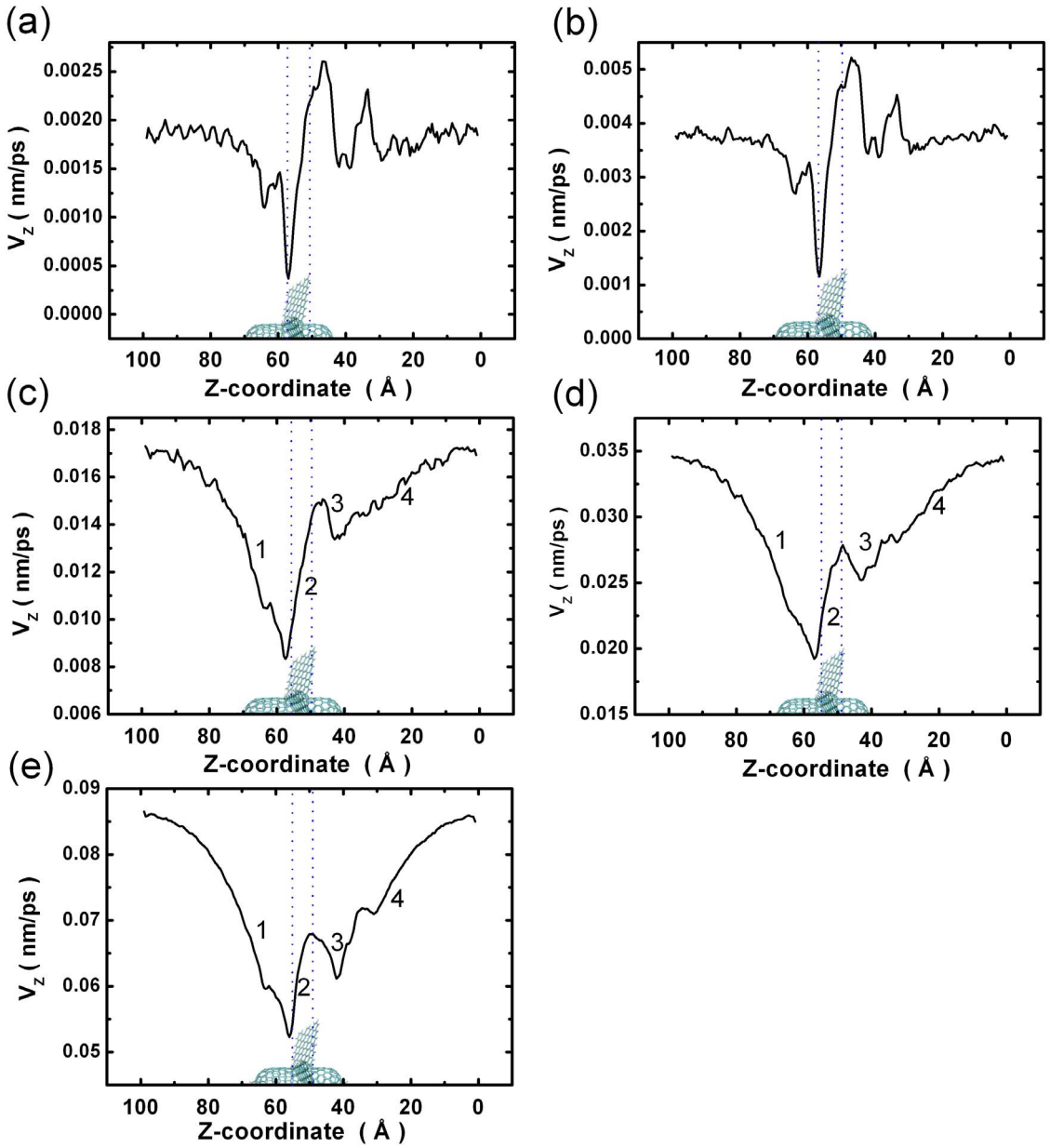

Figure 6 | The distribution of $V_{Z,locab}$ along the z-axis in the systems with the flow velocity of -1.82×10^{-3} (A), -3.63×10^{-3} (B), -1.8×10^{-2} (C), -3.56×10^{-2} (D), -8.9×10^{-2} nm/ps (E). All the distributions are similar to the distribution shown in Fig. 5. The water flow is disturbed in the region of 100 Å $<$ z $<$ 57 Å, and in the region immediately below the blade (57 Å $<$ z $<$ 48 Å) the water molecules are accelerated by the rotation of nano-turbine.

much larger than the slope from the above linear fit for the nano-turbine. Here we introduce a *slowing factor* α to characterize this discrepancy, with $\alpha = \omega/\omega_i = 0.064$. The rotation rate of the nano-turbine appears to be much slower ($\sim$15$\times$) than its macroscale analogue. As indicated by the macroscopic turbine flow meter, the discrepancy of actual rotation speed from the ideal rotation speed is less than 8 %[29].

Mechanisms of the Rotational Behavior of Nano-turbine. It is well accepted that the thermal noise is profound in the microscopic environment. The extent of thermal motion of water can be orders of magnitude larger than the actual flow velocity in our systems. In order to address the question on how the designed nano-turbine can still rotate largely unidirectionally when the flow velocity is relatively small, we first calculated the instant-average velocity of water by averaging the velocity of water molecules within a slab, with the size of the slab chosen as the blade size and the thickness of the slab 2 Å. As depicted in Fig. 1, the 2-Å slab is immediately above turbine blade, with same tilt angle as the blade. The instant-average water velocity is highly fluctuating even after averaging. Here we examine the system with the flow velocity of 1.82×10^{-3} nm/ps as an example. The width of the distribution of instant-average water velocity is 5.93×10^{-2} nm/ps, which is still more than one order of magnitude larger than the flow velocity (Fig. 3a). The direction of water flow flips frequently. The probability of having instant-average velocity of water along -z direction is only 53%, barely larger than the probability of being along the opposite +z direction. However the nano-turbine rotates largely unidirectionally (according to a net force from –z direction water flow), in counterclockwise direction rather than in highly random manner. The amplitude of the

fluctuation of rotation angle (the extent of rotating backward) keeps less than 10 degree in all the systems (Fig. S4), even though the frequency of rotating backward is large when flow velocity is small (the frequency can be more than 140 ns^{-1} when the flow velocity is 1.82×10^{-3} nm/ps). The relationship of the frequency of net rotation and the flow velocity can be fitted to a linear function very well (see Fig. S5). In summary, the relative fluctuations of the rotational motion are considerably smaller than the thermal fluctuation of the water velocity.

We further calculated the averaged velocity of water molecules within the 2 Å thick slab over a period of time, denoted by time-averaged water velocity. As one can expect, the fluctuation of time-averaged water velocity becomes smaller than the instant-average velocity of water. As the averaging window size increases, the fluctuation is further depressed and the peak of the distribution of time-average water velocity gets sharper. Thus, the probability of having time-averaged water velocity in the forward direction increases. For the system with the flow velocity of 1.82×10^{-3} nm/ps, the probability of time-averaged water velocity being along -z direction increases to 74 % as the window size increases to 50 ps (Fig. 3b). The direction of time-average water velocity is then dominated by the averaged water flow, and the effect of seemingly large thermal fluctuation vanishes. It is important to note that the windows size of 50 ps is still much smaller than the rotational period of the designed nano-turbine (more than 12 ns). Similar trends can be observed in the behavior of the net driving force to the nano-turbine (interested readers can refer to supplemental material for more details). As such, the rotational motion of the nanoscopic turbine maintains largely unidirectional, as shown in Fig. 2. Taken together, much smaller fluctuation of the rotational motion can be attributed to the time-and-space averaging.

It is important to note that the blade of our current nano-turbine is larger than that of most previously studied molecular rotary motors[16–21,30–32]. And we found that for even smaller nano-turbines the impact of thermal fluctuations on the rotation behavior will be more profound (see more discussion in supplementary material and Fig. 4). The rotation of even smaller nano-turbines may not be effectively driven by the fluid flow. The choice of the size of the nano-turbine, especially the blade size, thus is crucial to achieve a reliable performance of nano-turbines.

To further study the driving mechanism of rotation of the nano-turbine, we analyzed the velocity distribution of the water molecules in the region close to the nano-turbine (the cylinder region along nano-turbine axis with the radius of 21 Å). Here we use the system with the flow velocity of 8.63×10^{-3} nm/ps as an example. As shown in Fig. 5 the water velocity ($V_{Z,local}$) is remarkably different along the z-axis, while such dramatically fluctuating velocity distribution will be almost completely smoothed out in macroscopic turbine flow meter. The distribution of $V_{Z,local}$ can be divided into four regions. In the region above the turbine blade (region 1), the water velocity declines as the water molecules get close to the blade. And the average velocity of water directly above the blade ($V_{Z,local}$ at $z = 57$ Å), i.e. the effective driving flow velocity, is 2.98×10^{-3} nm/ps, only 34% of the bulk value. In the region corresponding to the blade (region 2) the average water velocity grows sharply to 9×10^{-3} nm/ps. And then the average water velocity relaxes to 6.9×10^{-3} nm/ps in the region of 48 Å $> z >$ 37 Å (region 3) before it finally converges to the bulk average value of 8.63×10^{-3} nm/ps (region 4).

The decrement of $V_{Z,local}$ in the *region 1* can be related to the much slower rotation rate of the nano-turbine. Again, we use the ratio of effective driving flow velocity to the bulk water velocity to characterize the effect of the disruption of water flow above the blade. Now consider the flow velocity and the broad distribution of individual water velocities within a 2-Å water slab, there is a considerable portion of water molecules whose velocities are larger than the velocity of the rotation of nano-turbine. Thus these water molecules bounce back from the upper surface of turbine blade, and disturb the water flow in the region above. The orientation of water molecules may be affected as well[33]. On the other hand, the water velocity sharply increases in *region 2*. The acceleration partly comes from the momentum exchange with the bulk water which has larger average velocity. However, the change in *region 2* is more dramatic than in *region 4* which is also due to the momentum exchange with the bulk water. Therefore, there should be another source for the acceleration. As discussed above, the distribution of velocity of individual water molecules is very broad, and there should be also a considerable portion of water molecules whose velocities are smaller than the velocity of the rotation of the nano-turbine or even moving along the opposite direction. Thus, these water molecules under the blade are pushed forward by the blades, and that also contributes to the acceleration in *region 2*. In other words, the rotation motion of nano-turbine is dragged by the water molecules below the blade, i.e. the dragging effect on the rotation motion. Besides, water exhibit considerable slippage at graphene surface[34–38], therefore, these water slippage also contribute to the much slower rotation motion. It should be noted that the slippage of water molecules can also be attributed to the hydrophobicity of graphene blade. Hence, the rotation rate of nanoturbine (i.e. the efficiency of converting energy) should be affected by the degree of hydrophobicity of graphene blade.

As suggested by the dramatically fluctuating velocity distribution, the much slower rotation rate of the nano-turbine can be attributed to several effects, including water flow disruption and the dragging effect, together with the water slippage at graphene surface. Consequently, the rotation rate of the nano-turbine is much slower than the macroscopic counterpart, where the rotation motion is close to the ideal case driven by the homogeneous water flow, and can be described with a simple geometric transformation of water flow velocity. The discrepancy of actual rotation speed from the ideal rotation speed is less than 8 %. And there should be an upper limit of efficiency for the nano-device converting the energy from fluid flow energy to the rotational motion.

Similar distributions of the velocities of water molecules in the vicinity region of nano-turbine are observed in the systems with different flow velocities (Fig. 6). The effective driving flow velocities (the average velocity of water directly above the blade) of all six systems are 2.91×10^{-4}, 1.05×10^{-3}, 2.98×10^{-3}, 8.46×10^{-2}, 1.96×10^{-2}, 5.34×10^{-2} nm/ps, respectively. Unlike the constant slowing factor $\alpha = 0.064$, the ratio of effective driving velocity to bulk value increases from 0.16 to 0.6 as the flow velocity increases (Fig. 7).

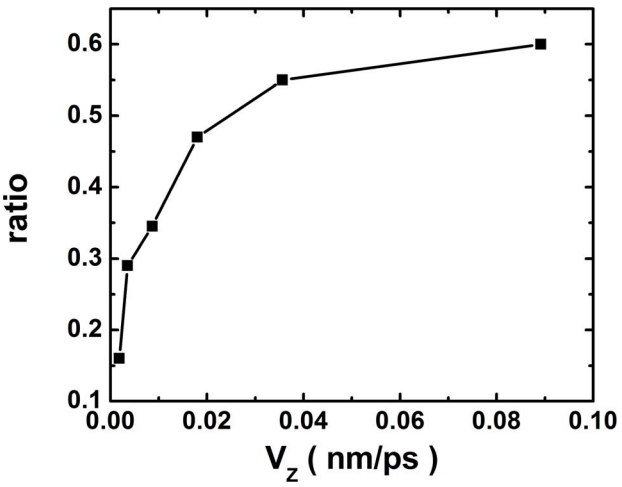

Figure 7 | The ratio of effective driving flow velocity to the bulk value as a function of the flow velocity. As the flow velocity increases, the extent of flow disruption decreases.

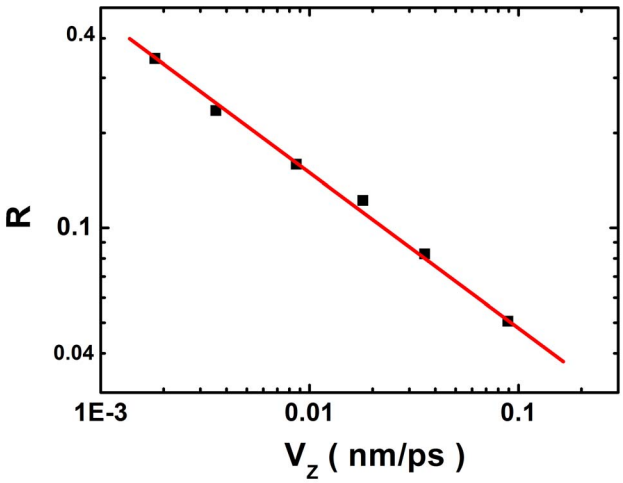

Figure 8 | The fluctuation of rotation period is characterized by the ratio of the standard deviation to the average value of rotation period. The relationship between them can be fit to the reciprocal of square root function, $R = 0.15 \times V_Z^{-0.5}$ (red curve).

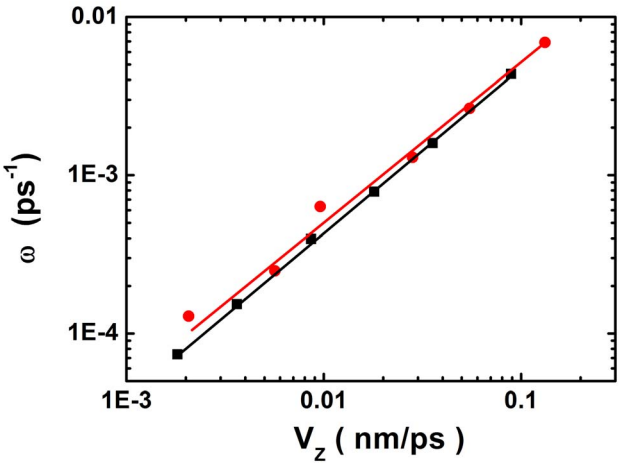

Figure 9 | The relationship of the flow velocity and rotation rate in 300 K (black) and 360 K (red).

The disruption of the water flow in *region 1* becomes less significant when the rotation rate increases. While the linear relationship between rotation rate and flow velocity remains intact, implying that the other effects such as the dragging and water slippage may become more profound as the rotation rate increases. On the basis of this robust linear relationship, the slowing factor α can then serve as the characteristic of the nano-turbine. It should be noted that the estimate of the efficiency of energy conversion is based on the idealized free-standing nano-turbine, the efficiency would become even smaller if it is loaded with a resistive coupler. And there should be an upper limit of efficiency for a given nano-device converting the energy from fluid flow energy to the rotational motion. These findings may serve as a foundation for the further development of nano-turbine to improve the efficiency of energy conversion.

Besides the much slower rotation rate, the rotation of nano-turbine fluctuates in the largely noisy environment especially when the flow velocity is relatively small. As the flow velocity increases, such fluctuation of the rotation period decreases. Here we calculated the relative ratio of the standard deviation of the rotation period to the average rotation period to characterize the extent of fluctuation. As shown in Fig. 8, the ratio decreases as the flow velocity increases. The relationship between the ratio and the average water velocity can be fit to the reciprocal of square root very well, $R = 0.15 \times V_Z^{-0.5}$. The relationship can be explained in terms of the law of large numbers about uncorrelated variables or events. For the number of water molecules within a small region (i.e. the hydration shell of the blade) the ratio of the standard deviation to the mean value of the number is proportional to the reciprocal of square root of the mean value. The fluctuation of rotation motion of nano-turbine largely arises from the fluctuation of average velocity of water molecules which directly interact with the blade. Such fluctuation is thus related to the fluctuation of the number of incoming water molecules with a given velocity. And the average rotation rate is proportional to the average flow velocity and hence the mean number of the incoming water molecules. As a result, the ratio of the standard deviation to the average rotation period follows a similar behavior to the number of the incoming water molecules, which is linearly proportional to the flow velocity Vz, i.e., $R \sim <N>^{-0.5} \sim Vz^{-0.5}$.

We also studied the rotation of nano-turbine at different temperature, i.e. 360 K. The viscosity of water decreases as the temperature increases[39]. Besides, the water velocity distribution become broader at 360 K (Fig. S7). We found the linear relationship between the water velocity and the rotation rate at 360 K is very close to that of 300 K (Fig. 9). While it should be noted that both relationships between (i) the driving force (the force of water exerting on the turbine blade) and the flow velocity, and (ii) the rotation rate and the driving force, change considerably at 360 K as compared to 300 K (Fig. 10). This indicates that such robust linear dependence of the rotation rate on the flow velocity may be more complicated than intuitive thinking. The reliable linear dependence of the rotation rate on the flow velocity in various environments ensures the potential of nano-turbine acting as the flow-meter to measure the flow velocity in nanoscopic length scale.

Conclusions

In this work, we designed a nano-turbine that can rotate largely unidirectionally as driven by the directional water flow. Several features of the rotation motion of nano-turbine are observed on the basis of the simulation of this model system. The rotation rate increases linearly with the flow velocity through two orders of magnitude. Comparing to the macroscopic counterpart, the rotation rate of the nano-turbine is much smaller. As indicated by the dramatically fluctuating velocity distribution, much slower rotation rate can be attributed to several effects including the flow disruption, dragging effect, together with the slippage on graphene surface. Moreover, the ratio of effective driving flow velocity increases as the flow velocity increases, indicating the reduced overall disruption effect. It suggests that the other effects such as water slippage and dragging get profound concomitantly to ensure the stable linear relationship. Beside the much slower rotation motion, the nano-turbine is found to rotate back-and-forth in small time period (less than 1 ns) even though it moves forward in the long run. The fluctuation of the rotation period decreases as the average water velocity increases. The relationship between the extent of fluctuation and the average water velocity can be fit to a reciprocal of square root very well. Our results suggest the significance of thermal fluctuation on the rotary behavior of the nano-turbine. So the choice of a sufficiently large blade is important for the performance of the nano-turbine. These findings might provide some insight to the further development of rotary nano-devices and should help to achieve a better understanding of the function of biological molecular motors. We also studied the rotation motion of nano-turbine in different temperatures (i.e. 300 K and 360 K). The linear relationship remains intact at different temperature. In this way, this nano-turbine can not only harvest

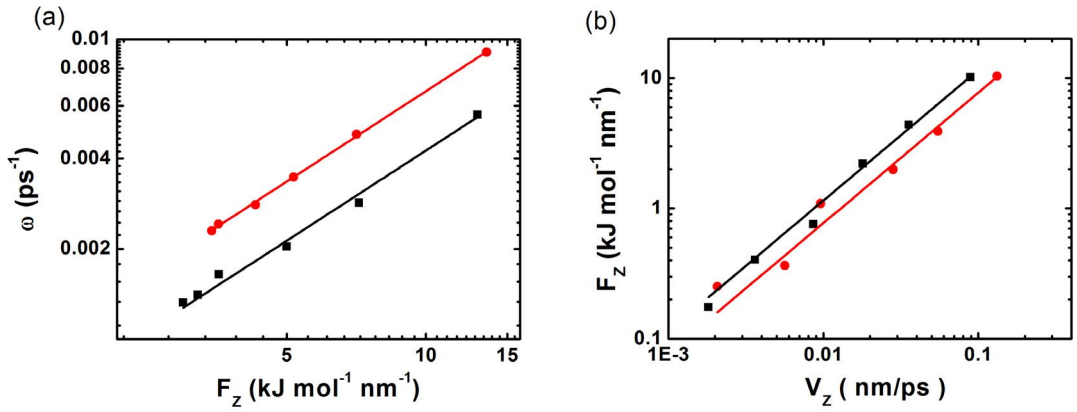

Figure 10 | The relationship among the flow velocity, driving force and rotation rate in 300 K and 360 K. (a) The dependence of the rotation rate on the driving force F_Z. With the same driving force, the nano-turbine rotates faster due to the smaller water viscosity at 360 K. (b) the relationship between the driving force and the flow velocity. Under the same flow velocity, the exerting force of water is smaller at 360 K because of smaller viscosity.

its energy from the flow environment, but also reliably detect its surrounding molecular flow.

1. Berg, H. C. Keeping up with F1-ATPase. *Nature* **394**, 324–325 (1998).
2. Abrahams, J. P., Leslie, A. G. W., Lutter, R. & Walker, J. E. Structure at 2.8 Å resolution of F1-ATPase from bovine heart mitochondria. *Nature* **370**, 621–628 (1994).
3. Noji, H., Yasuda, R., Yoshida, M. & Kinoshita, K. Jr. Direct observation of the rotation of F1-ATPase. *Nature* **386**, 299–302 (1997).
4. Dominguez, R, Freyzon, Y., Trybus, K. M. & Cohen, C. Crystal structure of a vertebrate smooth muscle myosin motor domain and its complex with the essential light chain: visualization of the pre-power stroke state. *Cell* **94**, 559–571 (1998).
5. Rayment, I. *et al.* Structure of the actin-myosin complex and its implications for muscle contraction. *Science* **261**, 58–65 (1993).
6. Magariyama, Y. *et al.* Very Fast Flagellar Rotation. *Nature* **371**, 752 (1994).
7. Shingyoji, C., Higuchi, H., Yoshimura, M., Katayama, E. & Yanagida, T. Dynein arms are oscillating force generators. *Nature* **393**, 711–714 (1998).
8. Bissel, R. A., Cordova, E., Kaifer, A. E. & Stoddart, J. F. A. Chemically and Electrochemically Switchable Molecular Shuttle. *Nature* **369**, 133–137 (1994).
9. Brouwer, A. M. *et al.* Reversible Translational Motion in a Hydrogen-Bonded Molecular Shuttle. *Science* **291**, 2124–2128 (2001).
10. Bedard, T. C. & Moore, J. S. Design and Synthesis of Molecular Turnstiles. *J Am Chem Soc* **117**, 10662–10671 (1995).
11. Khatua, S. *et al.* Micrometer-Scale Translation and Monitoring of Individual Nanocars on Glass. *ACS Nano* **3**, 351–356 (2009).
12. Kudernac, T. *et al.* Electrically driven directional motion of a four-wheeled molecule on a metal surface. *Nature* **479**, 208–2111 (2011).
13. Muraoka, T., Kinbara, K. & Aida, T. Mechanical Twisting of a Guest by a Photoresponsive Host. *Nature* **440**, 512–515 (2006).
14. Serreli, V., Lee, C.-F., Kay, E. R. & Leigh, D. A. A Molecular Information Ratchet. *Nature* **445**, 523–527 (2007).
15. Liu, Y. *et al.* Linear Artificial Molecular Muscles. *J Am Chem Soc* **127**, 9745–9759 (2005).
16. Horinek, D. & Michl, J. Surface-mounted altitudinal molecular rotors in alternating electric field: Single-molecule parametric oscillator molecular dynamics. *Proc Natl Acad Sci USA* **102**, 14175–14180 (2005).
17. Kelly, T. R., De Silva, H. & Silva, R. A. Unidirectional Rotary Motion in a Molecular System. *Nature* **401**, 150–152 (1999).
18. Leigh, D. A., Wong, J. K. Y., Dehez, F. & Zerbetto, F. Unidirectional Rotation in a Mechanically Interlocked Molecular Rotor. *Nature* **424**, 174–179 (2003).
19. Delden, R. A, V., Wiel, M. K. J. T., Pollard, M. M., Vicario, J., Koumura, N. & Feringa, B. L. Unidirectional Molecular Motor on a Gold Surface. *Nature* **437**, 1337–1340 (2005).
20. Zheng, X., Mulcahy, M. E., Horinek, D., Galeotti, F., Magnera, T. F. & Michl, J. Dipolar and Nonpolar Altitudinal Molecular Rotors Mounted on an Au(111) Surface. *J Am Chem Soc* **126**, 4540–4542 (2004).
21. Vacek, J. & Michl, J. Artificial Surface-Mounted Molecular Rotors: Molecular Dynamics Simulations. *Adv Funct Mater* **17**, 730–739 (2007).
22. Weiss, P. S. A molecular four-wheel drive. *Nature* **479**, 187–188 (2011).
23. Abrahamson, J. T. *et al.* Synthesis and Energy Release of Nitrobenzene-Functionalized Single-Walled Carbon Nanotubes. *Chem Mater* **23**, 4557–4562 (2011).
24. Huang, P., Zhu, H., Jing, L., Zhao, Y. & Gao, X. Graphene Covalently Binding Aryl Groups: Conductivity Increases Rather than Decreases. *ACS Nano* **5**, 7945–7949 (2011).
25. Li, J., Gong, X., Lu, H., Li, D., Fang, H. & Zhou, R. Electrostatic gating of a nanometer water channel. *Proc Natl Acad Sci USA* **104**, 3687–3692 (2007).
26. Tu, Y., Xiu, P., Wan, R., Hu, J., Zhou, R. & Fang, H. Water-mediated signal multiplication with Y-shaped carbon nanotubes. *Proc Natl Acad Sci USA* **106**, 18120–18124 (2009).
27. Xiu, P., Yang, Z., Zhou, B., Das, P., Fang, H. & Zhou, R. Urea-Induced Drying of Hydrophobic Nanotubes: Comparison of Different Urea Models. *J Phys Chem B* **115**, 2988–2994 (2011).
28. Hess, B., Kutzner, C., van der Spoel, D. & Lindahl, E. GROMACS 4: Algorithms for Highly Efficient, Load-Balanced, and Scalable Molecular Simulation. *J Chem Theory Comput* **4**, 435–447 (2008).
29. Stoltenkamp, P. W. Dynamics of turbine flow meters. PhD Thesis, Technische Universiteit Eindhoven (2007).
30. Fletcher, S. P., Dumur, F., Pollard, M. M. & Feringa, B. L. A. Reversible, Unidirectional Molecular Rotary Motor Driven by Chemical Energy. *Science* **310**, 80–82 (2005).
31. Kottas, G. S., Clarke, L. I., Horinek, D. & Michl, J. Artificial Molecular Rotors. *Chem Rev* **105**, 1281–1376 (2005).
32. Wang, B., & Kral, P. Chemically Tunable Nanoscale Propellers of Liquids. *Phys Rev Lett* **98**, 266102(266104) (2007).
33. Wang, C. *et al.* Stable Liquid Water Droplet on a Water Monolayer Formed at Room Temperature on Ionic Model Substrates. *Phys Rev Lett* **103**, 137801 (2009).
34. Falk, K., Sedlmeier, F., Joly, L., Netz, R. R. & Bocquet, L. R. Ultralow Liquid/Solid Friction in Carbon Nanotubes: Comprehensive Theory for Alcohols, Alkanes, OMCTS, and Water. *Langmuir* **28**, 14261–14272 (2012).
35. Kannam, S. K., Todd, B. D., Hansen, J. S. & Daivis, P. J. Slip length of water on graphene: Limitations of non-equilibrium molecular dynamics simulations. *J Chem Phys* **136**, 024705 (2012).
36. Xiong, W., Liu, J. Z., Ma, M., Xu, Z., Sheridan, J. & Zheng, Q. Strain engineering water transport in graphene nanochannels. *Phys Rev E* **84**, 056329 (2011).
37. Joly, L. Capillary filling with giant liquid/solid slip: dynamics of water uptake by carbon nanotubes. *J Chem Phys* **135**, 214705 (2011).
38. Joly, L., Ybert, C. & Bocquet, L. Probing the Nanohydrodynamics at Liquid-Solid Interfaces Using Thermal Motion. *Phys Rev Lett* **96**, 046101 (2006).
39. Brancker, A. V. Viscosity-temperature dependence. *Nature* **166**, 905–906 (1950).
40. Humphrey, W., Dalke, A. & Schulten, K. VMD: Visual molecular dynamics. *J Mol Graphics* **14**, 33–38 (1996).

Acknowledgments

This work was supported by CAS Hundreds Elite Program, MOST 973 programs (2013CB933704, 2012CB932504) and National Natural Science Foundation of China (NSFC) grant 21273240. R.Z. acknowledges the support from IBM Blue Gene Science Program.

Author contributions

J.L. and X.W. performed most of the simulations. J.L. and X.W. carried out most of the theoretical analysis. L.Z. carried out some theoretical analysis. J.L., X.G., Y.Z. and R.Z. contributed most of the ideas. J.L., X.W. and R.Z. wrote the paper. All authors discussed the results and commented on the manuscript.

Additional information

Supplementary information accompanies this paper at http://www.nature.com/scientificreports

Competing financial interests: The authors declare no competing financial interests.

How to cite this article: Li, J. *et al.* Rotation Motion of Designed Nano-Turbine. *Sci. Rep.* **4**, 5846; DOI:10.1038/srep05846 (2014).